ACTA NEUROBIOLOGIAE EXPERIMENTALIS

Acta Neurobiol Exp 2007, 67: 421–438

Distribution of the parvalbumin, calbindin-D28K and calretinin immunoreactivity in globus pallidus of the Brazilian short-tailed opossum *(Monodelphis domestica)*

Beata Domaradzka-Pytel[1], Katarzyna Majak[1], Jan Spodnik[1], Seweryn Olkowicz[2], Krzysztof Turlejski[2], Ruzanna L. Djavadian[2], and Janusz Moryś[1]

[1]Department of Anatomy and Neurobiology, Medical University of Gdańsk, 1 Dębinki St., 80-211 Gdańsk, Poland; [2]Department of Neurophysiology, Nencki Institute of Experimental Biology, 3 Pasteur St., 02-093 Warsaw, Poland

Abstract. This study describes the topography, borders and divisions of the globus pallidus in the Brazilian short-tailed opossum (*Monodelphis domestica*) and distribution of the three calcium binding proteins, parvalbumin (PV), calbindin D-28k (CB) and calretinin (CR) in that nucleus. The globus pallidus of the opossum consists of medial and lateral parts that are visible with Nissl or Timm's staining and also in PV and CR immunostained sections. Neurons of the globus pallidus expressing these proteins were classified into three types on the basis of size and shape of their soma and dendritic tree. Type 1 neurons had medium-sized fusiform soma with dendrites sprouting from the opposite poles. Neurons of the type 2 had medium-to-large, multipolar soma with scarce, thin dendrites. Cell bodies of type 3 neurons were small and either ovoid or round. Immunostaining showed that the most numerous were neurons expressing PV that belonged to all three types. Density of the PV-immunopositive fibers and puncta correlated with the density of the PV-labeled neurons. Labeling for CB resulted mainly in the light staining of neuropil in both parts of the nucleus, while the CB-expressing cells (mainly of the type 2) were scarce and placed only along the border of the globus pallidus and putamen. Staining for calretinin resulted in labeling almost exclusively the immunoreactive puncta and fibers that were distributed with medium-to-high density throughout the nucleus. Close to the border of globus pallidus with the putamen these fibers (probably dendrites) were long, thin and varicous, while more medially bundles of thick, short and smooth fibers predominated. Single CR-ir neurons (all of the type 3) were scattered through the globus pallidus. Colocalization of two calcium binding proteins in one neuron was never observed. The CB-ir puncta (probably terminals of axons projecting to the nucleus) frequently formed basket-like structures around the PV-ir neurons. Therefore, the globus pallidus in the opossum, much as that in the rat, consists of a heterogeneous population of neurons, probably playing diversified functions.

Correspondence should be addressed to B. Domaradzka-Pytel,
Email: bdp@amg.gda.pl

Key words: Monodelphis, marsupials, globus pallidus, parvalbumin, calbindin, calretinin, confocal microscopy

INTRODUCTION

The globus pallidus (GP), together with the entopeduncular nucleus, belong to the pallidal part of the basal ganglia. In coronal brain sections of many mammalian species GP is visible as a small, pyramid-shaped nucleus laterally bordering putamen and medially protruding into the internal capsule. At its medioventral border a small group of cells dispersed among fibers of the internal capsule forms the entopeduncular nucleus that is most prominent in primates (Kita 2007, Kita and Kitai 1994).

In the rat GP has been variably divided into medioventral and dorsolateral compartments (Hontanilla et al. 1998), or ventral lateral and dorsal portions (Haber et al. 1985). These parts are presumed to have differing projections. Some authors also distinguish a GP shell zone, on its border with the striatum (Gerfen et al. 1985). The primate equivalent of the whole GP in rodents is the lateral (or external) GP, while the medial (internal) part is formed by an expanded part of the entopeduncular nucleus (Gerfen 2004, Hardman et al. 2002, Kita 2007, Kita and Kitai 1994, Nambu 2007).

The GP is deeply involved in the exchange of information among the basal ganglia. Therefore, it plays an important role in movement regulation, but it also influences various adaptive behaviors, such as the induction of movements of the animal in response to novelty and supporting spatial working memory (Hooks and Kalivas 1995, Kalivas et al. 1999, Maurice et al. 1997, Xue et al. 2007) or participating in disgusting reactions to unpalatable food (Calder et al. 2007).

These functions of GP are supported by a wide range of connections and a heterogeneous population of cells. Connections of the rat GP and its primate equivalent, the lateral or external, according to nomenclature used by Gerfen 2004, Kita 2007, and Kita and Kitai 1994) part of GP share many similarities. GP is bilaterally connected with the striatum and other nuclei of the basal ganglia, such as the reticular part of substantia nigra and subthalamic nucleus, dorsal and ventral thalamic nuclei (suprageniculate nucleus, medial division of the medial geniculate nucleus, reticular thalamic nucleus, zona incerta), lateral hypothalamus, accessory optic nuclei and some regions of the midbrain, e.g. the pedunculopontine nucleus, inferior colliculus and the periaqueductal gray (Haber et al. 1985, Kincaid et al. 1991, Kita and Kita 2001, Kita and Kitai 1987, Moriizumi and Hattori 1992, Shammah-Lagnado et al. 1996, Smith and Bolam 1989). GP receives many cortical afferents, from the somatosensory, temporal, insular, orbital, prelimbic and perirhinal areas (Kita and Kita 2001, Naito and Kita 1994, Shammah-Lagnado et al. 1996, Stepniewska et al. 2007).

The striatal input to the lateral GP is inhibitory, GABA-ergic and enkephalinergic (Difiglia et al. 1982) whereas the main excitatory input is sent from the subthalamic nucleus (Kita and Kitai 1987). Dopaminergic innervation of GP arises from the substantia nigra and exerts an inhibitory influence on the GP neurons (Zold et al. 2007). In humans some segments of GP are innervated by axons containing substance P that terminate on cells expressing the neurokinin-1 receptor (Levesque et al. 2003). Efferents from the GP (mainly from its most medial part and also from the entopeduncular nucleus) end on the GABA-ergic interneurons of the striatum and substantia nigra (Bevan et al. 1998, Haber et al. 1985, 1993, Kita and Kitai 1994).

Electrophysiological, immunohistological and morphological studies showed that the GP of the rat is composed of a histologically and functionally heterogeneous population of neurons. A large majority of the projection neurons of GP are GABA-ergic but they belong to various morphological types differing also in their connectivity (Difiglia and Rafols 1988, Sadek et al. 2007). These neurons were classified into two types: spinous and aspinous, which correlated with some other differing characteristics (Kita and Kitai 1994). A scarce population of cholinergic neurons has also been observed in the GP (Ingham et al. 1985, Grove et al 1986) while other neurons may express proenkephalins (Hoover and Marshall 2002). Also on the basis of the electrophysiological activity the GP neurons were classified into several types (Nambu and Llinas 1994).

In marsupials the basal ganglia have been described morphologically only in the Didelphis opossum (Bodian 1940, Loo 1930, 1931, Martin and Hamel 1967, Pilleri 1962, Schnitzlein et al. 1973), but even in that species there is no report of the results of investigations with modern techniques of axonal transport or immunocytochemistry. In *Didelphis virginiana* the GP borders the same anatomical structures as in Eutheria, but it is relatively smaller than in rodents and shows

no apparent segmentation in the Nissl-stained sections, although its volume is traversed by bundles of fibers (Martin and Hamel 1967, Pilleri 1962, Schnitzlein et al. 1973). Many of its cells are large and stain intensely in the Nissl procedure (Martin and Hamel 1967, Schnitzlein et al. 1973). Very little is known about connections of the GP in Didelphis, only the caudate projection to GP has been documented in that species with the degeneration techniques (Mickle 1976). The entopeduncular nucleus of Didelphis consists of a scarce cellular population scattered among fibers of the internal capsule (Schnitzlein et al. 1973). The only other marsupial species where the gross morphology of the basal ganglia has been described (including a short description of GP) is the kangaroo (Hamel 1996).

The calcium binding proteins (CaBPs) that are expressed in neurons belong to the EF-hand family of calcium-modulating proteins. Their main role is buffering intracellular calcium ions (Ca^{+2}) that have a wide variety of intracellular functions including the release of neurotransmitters and hormones, microtubular transport and triggering various enzymatic reactions (Burgoyne 2007). Abnormally high levels of intracellular Ca^{+2} may lead to severe cell dysfunctions or even death (for review see Bano and Nicotera 2007). Disturbances in the intracellular levels of Ca^{+2} have been implicated in the pathogenesis of many neurodegenerative diseases (for reviews see Heizmann and Braun 1992, Mattson 2007). Differential expression of several CaBPs in various brain structures is frequently used as a tool for delineating borders of these structures (Badowska-Szalewska et al. 2005, Celio 1990, Cheng et al. 2003, FitzGibbon 2000, Hof et al. 1999, Jones 2007, Resibois and Rogers 1992, Wojcik et al. 2006). Beginning of expression of some CaBPs at certain time points during development is also used to assess the developmental stage of structures of the nervous system (Barker and Dreher 1998).

Distribution of such CaBPs as parvalbumin (PV), calbindin D-28k (CB) and calretinin (CR) in the nervous system of the rat and primates has been widely studied (for review see Hontanilla et al. 1998, Parent et al. 1996). Several studies described distribution of the CaBP within the GP of the rat (Cooper and Stanford 2002, Hardman et al. 2002, Hontanilla et al. 1998, Rajakumar et al. 1994) and in the external part of GP of monkeys and humans, corresponding to the whole GP in the rat (Adams et al. 2001, Cote et al. 1991, Hardman et al. 2002, Kalanithi et al. 2005, Morel et al. 2002, Parent et al. 1996, Waldvogel et al. 1999, 2004). Cells expressing PV were found to have broad projections to many structures, while the PV-negative cells projected only to the subthalamic nucleus (Kita and Kitai 1994). There are only a few descriptions of CaBPs distribution in the marsupial brain (Dino et al. 1999, Jia and Halpern 2004) and none of them concerns the basal ganglia.

The Brazilian short-tailed opossum, *Monodelphis domestica*, is a small marsupial showing many brain features that are either primordial for mammals or typical for marsupials (Beck et al. 1996, Karlen and Krubitzer 2007, Lende 1963a,b, Pubols et al. 1976, Saunders et al. 1989). For example, in marsupials there is no corpus callosum and the motor and somatosensory cortical representations overlap (reviewed by Frost et al. 2000, Heath and Jones 1971, Rowe et al. 1981). Moreover, the motor cortex of the Monodelphis is the smallest of those in the investigated mammalian species and encompasses only a representation of the head and neck (Frost et al. 2000, Karlen and Krubitzer 2006). Because of a very precocious stage of development of the newborn opossum pups, this species is frequently used in developmental studies (Djavadian et al. 2006, Krause and Saunders 1994, Saunders et al. 1989). However, data about expression of CaBPs in the brain of the Monodelphis are scarce (Dino et al. 1999, Jia and Halpern 2004) and there is no description of its basal ganglia.

The purpose of the present study was a description of the morphology and histology of the GP in the Brazilian short-tailed opossum, (*Monodelphis domestica*). For this purpose we used several histological techniques (Nissl and Timm's staining, staining for the acetylcholinesterase) and the immunohistochemical labeling for the presence of three CaBPs: parvalbumin, calbindin and calretinin that showed their differential expression in the opossum GP. This is the first report on the histology of GP in the Monodelphis and on the distribution of the CaBPs in the basal ganglia of marsupials. Comparison of our data with those for the rat and primates allows better assessment of homologies in the GP anatomy and histology among mammalian species. It also allows some conclusions to be drawn about functional homologies and differences of GP in various mammalian species.

METHODS

Animals

All experiments were approved by the Local Committee for the Ethics of Animal Experimentation and conducted in accordance with the Polish law and the Guidelines of the European Community Council Directive 86/609/EEC. Brains of five male and five female adult Monodelphis opossums (*Monodelphis domestica*, weight 73–124 g, raised in the Animal Center of the Nencki Institute of Experimental Biology, Warsaw, Poland) were used in this study. Sections from brains of three animals were used for the single immunostaining for the presence of PV, CB and/or CR. Four other brains were used for double-labeling for these proteins. Two more animals were used for the Timm's method and one for staining for acetylcholinesterase.

For all stainigs except of the Timm's method, brains of the deeply anesthetized animals (Thiopental, 100 mg/kg, i.p.) were initially flushed transcardially with the phosphate buffered saline (PBS) and then perfused with 4% paraformaldehyde in the 0.1 M phosphate buffer (PB) at 4°C. Subsequently, the brains were removed, post-fixed for 2 h in the perfusing solution and then cryoprotected by immersion in 30% sucrose for 24 h at 4°C. Next, the brains were cut into 40 μm sections, coronal (7 brains) or horizontal (3 brains), on a cryostat (Jung CM1800, Leica, Germany). Sections were collected on glass slides and stored at –20°C until further processing.

Animals used for the Timm's staining (for the presence of synaptic vesicular zinc) were initially perfused first with 0.1% Na_2S in PB, then with 3% glutaraldehyde solution in PB and then again with Na2S solution in PB. After perfusion brains were briefly postfixed (30 min) in the same glutaraldehyde solution as used for perfusion, cryoprotected and cut in the horizontal plane on a cryostat.

Histology

To asses the cytoarchitectonic boundaries of the GP, sections from seven brains (series of every 6th section) were stained with 10% cresyl violet. Sections used for the Timm's method were collected on gelatinized slides and further processed as described by Danscher (1981).

For the acetylcholinesterase stain free-floating sections were incubated for 3–5 hours in the following solution: 0.002 M $CuSO_4 \times 5H_2O$, 0.01 M glycine, 0.105 M acetic acid and 0.29 M sodium acetate, adjusted to pH 5. Just prior to incubation 1160 mg of acetylthiocholine iodide and 60 mg ethopropazine per 1 liter of the solution were added. Then, sections were rinsed 6 times in water and developed for 60 seconds in 1.25% solution of sodium sulfide (pH adjusted to 7.5 with HCl). Sections were then rinsed with water 6 times and the colored precipitate was intensified in 1% $AgNO_3$ solution for 60 seconds. Rinsed again 3 times in water and differentiated in sodium thiosulfate (5% in water), they were next rinsed in water, mounted from PB onto slides, dried and coverslipped.

Immunohistochemistry

The remaining coronal series of sections were single or double-labeled with standard immunohistochemical protocols using antibodies against the three investigated CaBPs. Briefly, after 3 washings (15 min each) in PBS, they were blocked in 5% normal goat serum and 0.3% Triton X-100 for 2.5 h at room temperature. For single staining these sections were incubated with the solution of a primary antibody solution (either 1:2000 monoclonal anti-parvalbumin raised in mouse, #P3088 Sigma, Germany, or 1:2000 monoclonal anti-calbindin D-28K raised in mouse, #C9848, Sigma, or 1:1500 polyclonal anti-calretinin raised in rabbit, #AB5054, Chemicon, Temecula, CA, USA) for three days at room temperature. Then the sections were washed 3 times for 15 min in 0.01 M PBS and incubated for 2.5 h at room temperature with the secondary antibodies: 1:600 goat anti-mouse conjugated with the Cy3 fluorescent dye (#115-165-146, Jackson ImmunoResearch Laboratories, West Grove, PA, USA) for PV or CB and 1:600 goat anti-rabbit conjugated with Cy3 (#111-165-144, Jackson ImmunoResearch Laboratories for calretinin) for CR.

For double staining, sections were first incubated with a cocktail of primary antibodies (1:1500 anti-parvalbumin raised in mouse and #P3088, Sigma and 1:1000 polyclonal anti-calbindin D-28K raised in rabbit, #AB1778, Chemicon, or 1:1500 anti-parvalbumin raised in mouse, #P3088 Sigma and 1:1500 polyclonal anti-calretinin raised in rabbit, #AB5054, Chemicon, or 1:1000 monoclonal anti-calbindin D-28K raised in mouse, #C9848, Sigma and 1:1500 polyclonal anti-calretinin raised in rabbit, #AB5054, Chemicon). Then the sections were washed 3 times in 0.01 M PBS for 15 min and incubated with one of the two cocktails of secondary antibodies conjugated with the fluorescent dyes: 1:600 goat anti-mouse Cy3 (#115-165-146, Jackson ImmunoResearch

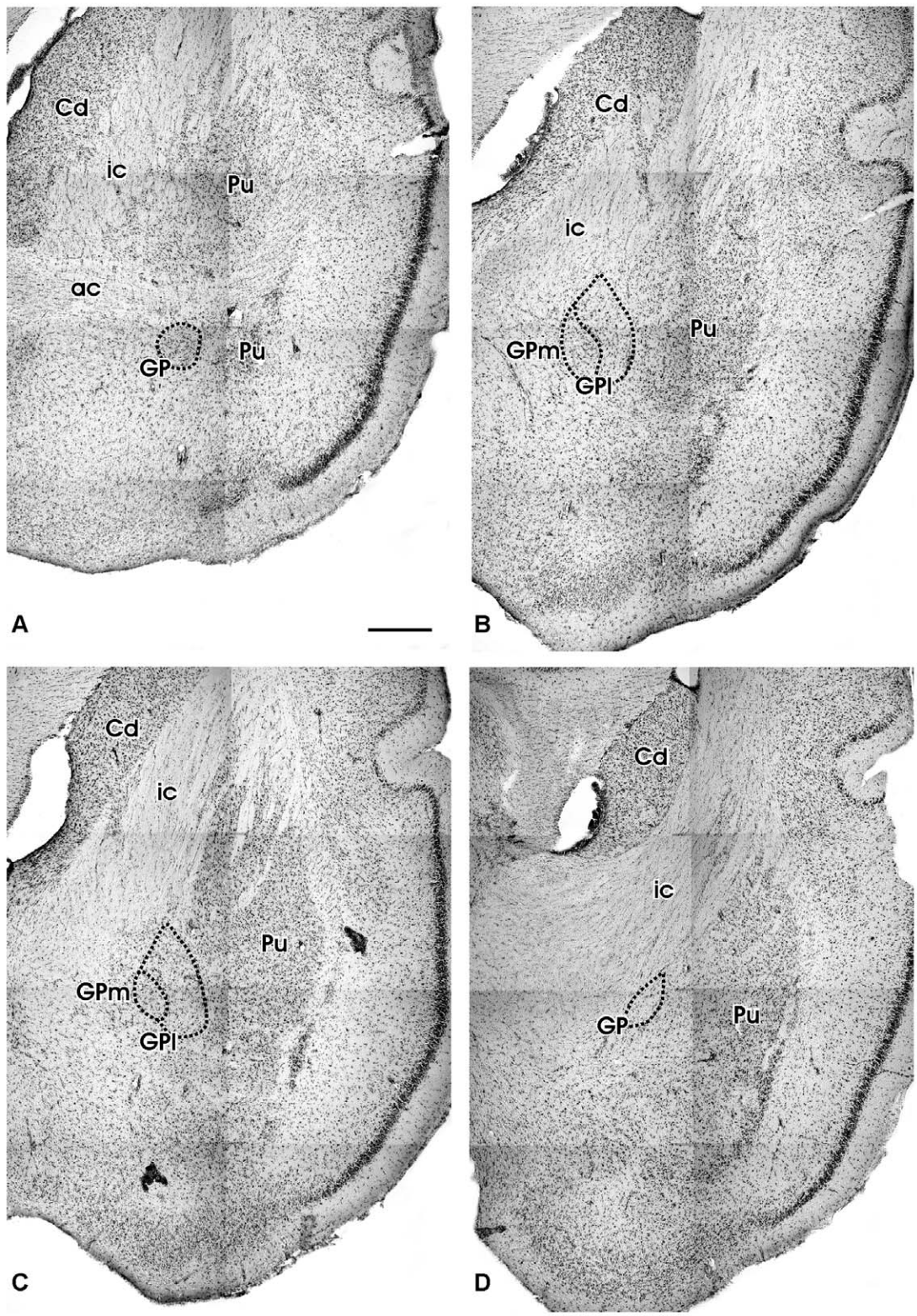

Fig. 1. Brightfield photomicrographs of cresyl violet-stained coronal sections of the Monodelphis opossum brain showing the location and cytoarchitectonics of the globus pallidus and its parts. Dotted lines show borders of GP and its lateral and medial parts (GPl and GPm). Section (A) is the most rostral and (D) is the most caudal. Scale bar in (D) equals 500 μm and applies to (A)–(D).

Laboratories) and 1:600 goat anti-rabbit Cy3 (#111-165-144, Jackson ImmunoResearch Laboratories) or 1:150 goat anti-mouse Alexa Fluor 488 (A-11001, Molecular Probes, Eugene, OR, USA) and 1:150 goat anti-rabbit Alexa Fluor 488 (#11008, Molecular Probes) for 2.5 h at room temperature. Finally, the sections were washed, mounted on slides and coverslipped with Kaiser's Glyceringelatine (#A12083, Merck, Germany).

Specificity of the immunostaining was checked by omitting either the primary or secondary antibodies which resulted in total disappearance of the staining. We also used two different types of the secondary antibodies: conjugated with either Cy3 or Alexa Fluor 488 fluorochromes for each primary antibody. In all cases results of labeling were similar.

Analysis of the labeled sections

GP and its boundaries were identified and drawn on pictures taken from the adjacent thionin-stained sections and superimposed on top of the fluorescent pictures. The immunolabeled sections were analyzed using a fluorescent microscope (Olympus BX51, Japan) and a confocal system (BioRad Radiance 2100, UK) equipped with the krypton/argon laser as well as with the light/fluorescent microscope Eclipse 600 (Nikon, Japan). The image analysis program Laser Sharp 2000 v.4.0 (BioRad) was used for the confocal image reconstruction and Color View II (Nikon) for fluorecent and light microscope image reconstruction.

The density of the labeled cells was assessed semi-quantatively as follows: (-) no cells; (+) scarce (cf. Fig. 5C); (++) moderate density (cf. Fig. 4A); (+++) high density (cf. Fig. 4C). The density of neuropil labeling (fibers and immunoreactive points) was assessed as follows: (•) sparse (cf. Fig. 5C); (••) medium density (cf. Fig. 4L); (•••) dense (cf. Fig. 4K).

The size of cell bodies of the various types of PV-ir cells was measured on CLSM images using the Leser Pix 2.0 analyzer (BioRad, UK). Over 100 PV-ir cell bodies of each type were measured for these estimations. Cells expressing CB or CR were too scarce to be used in this analysis. We measured the square area of a cell body and its diameters (long and short).

List of abbreviations

AB	accessory basal nucleus of amygdala
ac	anterior commissure
CaBP	calcium binding protein
CB	calbindin D28K
Cd	caudate nucleus
CR	calretinin
GP	globus pallidus
GPm	medial part of globus pallidus
GPl	lateral part of globus pallidus
ic	internal capsule
Pu	putamen
PV	parvalbumin
PV-ir	immunoreactivity or immunoreactive to parvalbumin
CB-ir	immunoreactivity or immunoreactive to calbindin
CR-ir	immunoreactivity or immunoreactive to calretinin

RESULTS

Nomenclature, placement and divisions of the GP

Since no cytoarchitectonic brain atlas is available for the *Monodelphis* opossum, brain structures were identified with the help of atlases of the brain of the *Didelphis aurita* opossum (Oswaldo-Cruz and

Fig. 2. Photomicrographs of horizontal sections of the opossum brain showing basal ganglia, including the globus pallidus (GP) stained with several histochemical methods. For each method sections through the dorsal level are in the top row, intermediate in the second and ventral in the third row. In all pictures rostral is at the top and lateral to the left. In the Nissl-stained sections (A)-(C) GP is visible as a separate nucleus medially to the putamen. Clear cytoarchitectural differences between these nuclei are visible under higher magnification [in (D) putamen, in (H) globus pallidus, magnified from boxes in (B)]. Borders between the globus pallidus (GP) and putamen (Pu) are most clearly visible in sections stained with Timm's method for synaptic vesicular zinc (E)–(G). Lateral and medial subdivisions of GP (GPl and GPm) are visible in sections cut through the middle part of the nucleus (F). In sections stained histochemically for acetylcholinesterase (I-K) GP stains somewhat darker than putamen. On the section immunostained for calretinin (L) that cuts across the ventral level of GP and probably contains only GPl, GP is well demarcated from putamen because of its uniform, moderate level of immunolabeling. Scale bar in (L) equals to 1 mm and applies to all pictures except of (D) and (H). The scale bar in (H) equals 100 μm and applies to (D) and (H).

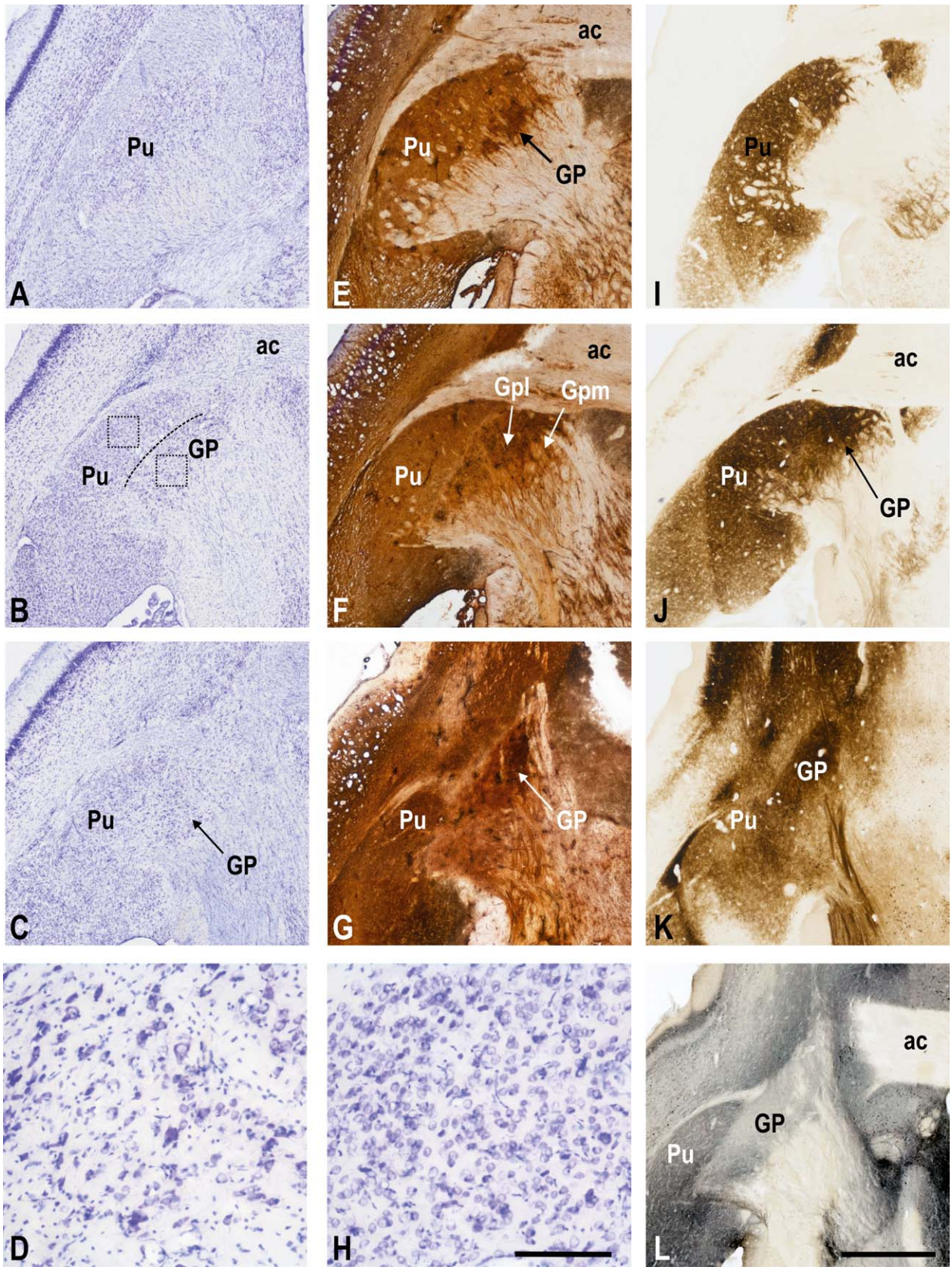

Fig. 2. For explanations see page 6

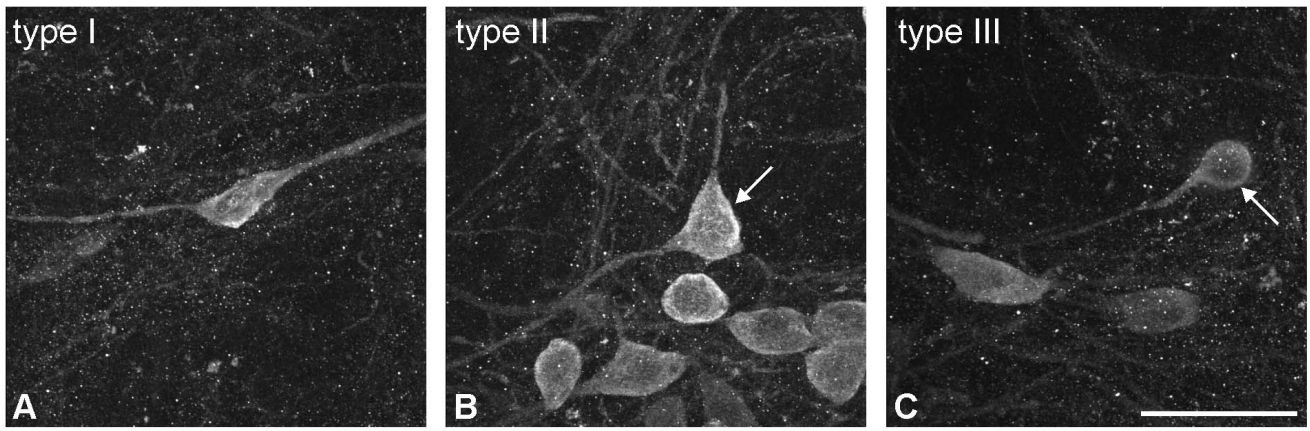

Fig. 3. Confocal photomicrographs of three cell types stained for parvalbumin (A)–(C). (A) Type 1 neuron with medium-size fusiform soma spreading dendrites from opposite poles; (B) Type 2 neuron (arrow) with medium-to-large multipolar cell body and dendrites of variable thickness; (C) Type 3 neuron (arrow) with mall, ovoid or round soma. Scale bar in (C) equals 25 μm and applies to (A)–(C).

Rocha-Miranda 1968) and rat (Paxinos and Watson 1998). As in other mammals, in the Monodelphis GP is visible in the Nissl-stained coronal and horizontal sections of the brain as a well-delineated nucleus placed medially to putamen (Pu, Figs 1 and 2A–C). Cytoarchitectonic differences between these two nuclei were clearly visible under higher magnification (Fig. 2D,H). Medially and ventrally the GP borders the anterior limb of the internal capsule (ic) and its sublenticular portion respectively. Therefore, GP in Monodelphis borders the same structures as in Didelphis (cf. Martin and Hamel 1967). At the ventro-medial corner of GP, among the ic fibers there is a sparse population of cells forming a rudiment of the entopeduncular nucleus that in the Monodelphis is as inconspicuous as in the Didelphis (cf. Martin and Hamel 1967, Oswaldo-Cruz and Rocha-Miranda 1968). Ventrally to the GP and fibers of the ic lies the substantia innominata and the nucleus of the ansa lenticularis. In the rostro-caudal dimension, the opossum GP begins at the level of caudal-most aspect of the anterior commissure (Figs 1A and 2B) and ends at the level at which the accessory basal nucleus of amygdala (AB) begins (Figs 1D and 2B,C).

For partitioning of the opossum GP into the medial (GPm) and lateral (GPl) parts we adopted nomenclature used by Hontanilla and coworkers (1998) in the rat. Our GPm and GPl correspond respectively to the medioventral and dorsolateral parts of GP of those authors. In the most rostral and caudal parts of the GP we could distinguish only the GPl (Figs 1A,D and 2B). GPm was also absent in horizontal sections across the most dorsal and ventral levels of GP (Fig. 2A,C). Therefore, in the Monodelphis GPm was present only in the centro-medial part of GP.

On the Nissl-stained sections, both GPm and the GPl were found to be composed of a similar, heterogeneous population of neurons. However, in the GPm cells were packed more densely than in the GPl (Figs 1 and 2). Borders between the GP) and putamen (Pu) were also clearly visible in sections stained with the Timm's method (Fig. 2E–G). Lateral and medial subdivisions of GP (GPl and GPm) were visible at section cutting through the middle part of the nucleus (Fig. 2F). In sections stained histochemically for the presence of acetylcholinesterase (Fig. 2I–K) the GP stained somewhat darker than Pu but the border between these nuclei was not as clearly visible as in the Timm's staining. In a horizontal section across the ventral level of the GP that was immunostained for calretinin (Fig. 2L) GP was well demarcated from the surrounding structures because of its uniform moderate-to-weak level of immunolabeling. Therefore, in the Monodelphis borders of the GP and its parts may be delineated by several methods which yield the same results, confirming our delineation.

Morphological types of the CaBP immunoreactive neurons of the GP

In Nissl-stained sections the majority of GP cells displayed medium-to-large, predominantly triangular

somas and darkly staining, centrally located nucleus. Cells with large, oval cell bodies were also present but in lower numbers. Basing on the shape of cell body and the characteristics of the dendritic tree we distinguished three major neuronal types in the GP. Examples of these cell types, labeled with the PV immunohistochemistry, are shown in the Fig. 3. Type 1 neurons (Figs 3A and 6A) had medium-sized, fusiform somata (square area 192.9 ± 4.5 μm^2; dimensions 21.6 ± 0.4 × 12.2 ± 0.2 μm; mean ± SEM) with dendrites sprouting from the opposite poles. One of these dendrites was always thicker than the rest. Type 2 neurons (Fig. 3B) had medium-to-large, multipolar, predominantly triangular somata (square area 203.5 ± 5.5 μm^2; dimensions 19.8 ± 0.4 × 14.6 ± 0.2 μm) with few thin and poorly staining dendrites. Type 3 neurons

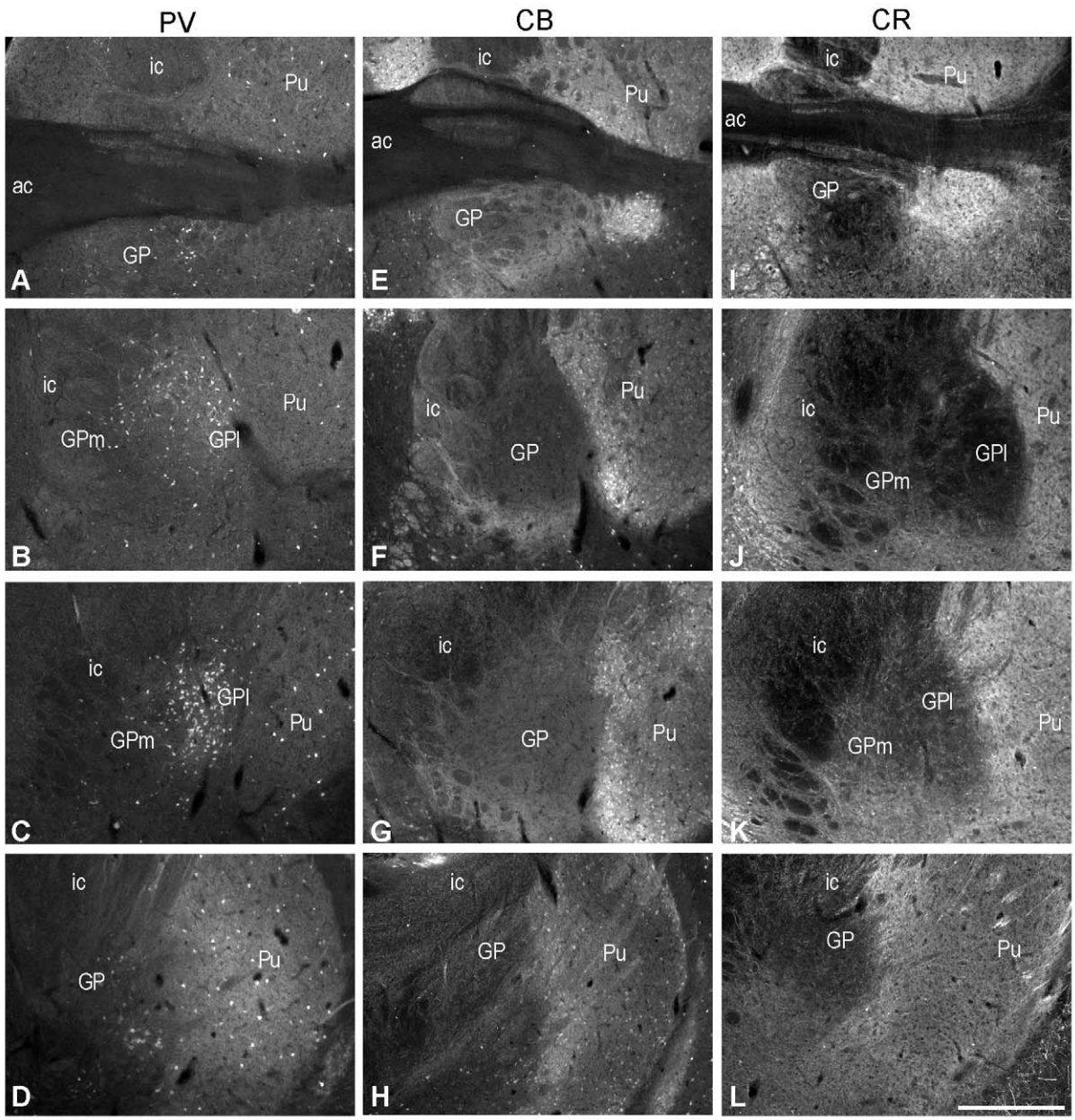

Fig. 4. Distribution of calcium binding proteins immunoreactivity in the Monodelphis GP. The fluorescent photomicrographs were taken at four levels presented in the Fig. 1. Panels (A), (E) and (I) in this figure correspond to the panel (A) in Fig. 1, panels (B), (F), (J) to the panel (B), panels (C), (G), (K) the panel (C), and panels (D), (H), (L) to the panel (D). PV-ir is presented in panels (A)–(D), CB-ir in panels (E)–(H) and CR-ir in panels (I)–(L). Scale bar in (L) equals to 500 μm and applies to (A)–(L).

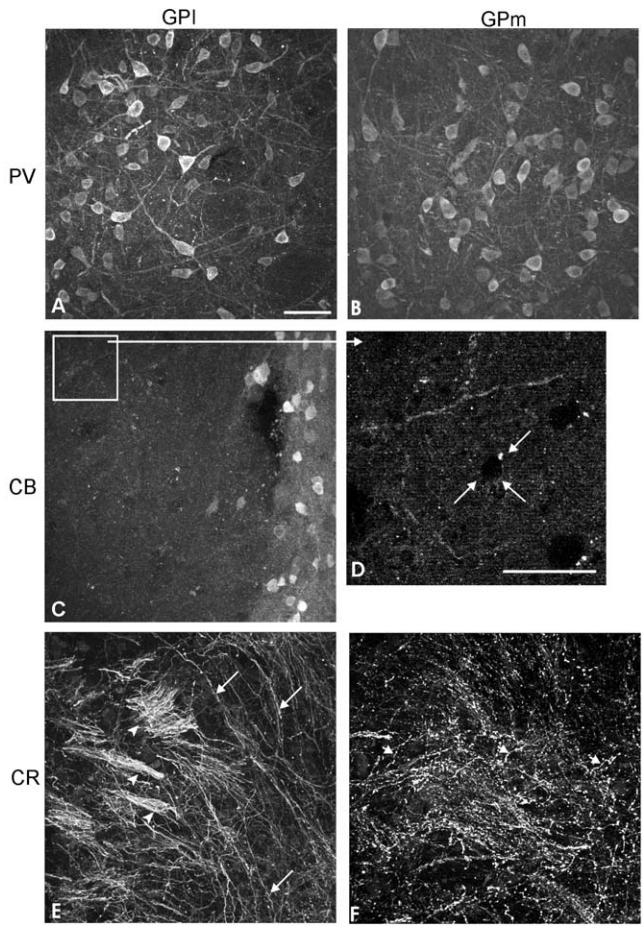

Fig. 5. Confocal photomicrographs demonstrating PV (A, B), CB (C, D) and CR (E, F) immunoreactivity of cells and neuropil in the lateral (A, C, E) and medial (B, F) parts of the globus pallidus. Arrows in panel (D) point to the long, thin and varicose fibers of GPl running along its border with the putamen. Arrowheads indicate bundles of thick, short and smooth fibers predominating in the more medial aspect of GPl. Arrows in panel (E) show short, thin and varicose fibers in GPm. Scale bar in (A) and (D) equal to 25 μm.

(Fig. 3C) had small, ovoid or round somata (square area 123.0 ± 5.3 μm^2; dimensions 14.5 ± 2.4 × 10.9 ± 0.3 μm) that typically were less intensely stained than in other neuronal types. Distribution and density of the PV-, CB- and CR-ir cells of various types and of the immunostained neuropil are described below and summarized in Table I.

Parvalbumin

PV-immunoreactivity (PV-ir) consisted of immunopositive cell somata, dendrites and immunoreactive puncta (Fig. 4A–D). Immunostaining for PV resulted in labeling of the highest numbers of neurons out of the three studied CaBPs. All three types of neurons were immunolabeled for PV (Figs 3 and 5A,B). Along the rostro-caudal axis, the highest density of the PV-ir cells was observed in the central part of GPl (Figs 4B,C and 5A), while at the anterior and posterior poles they were present in moderate densities (Fig. 4A,D). In the GPm the density of PV-ir cells was also classified as heavy, however, somata of cells in that subnucleus were less intensely stained than in the GPl and they clustered in the center of GPm (Figs 4B,C and 5B). Density of the immunopositive neuropil in general followed the same pattern. The majority of immunostained fibers were smooth and their density was higher in the GPm (Fig. 5B), whereas the immunoreactive puncta were evenly distributed within the GP.

Calbindin

CB-ir consisted almost exclusively of lightly stained neuropil distributed evenly throughout the entire rostrocaudal extent of both parts of GP (Fig. 4E–H). These were mainly immunoreactive puncta (Fig. 6B,C) that sometimes surrounded cells that did not themselves stain for CB (Fig. 5D). We observed also single, short, thin and smooth CB-ir fibers (Fig. 5D). Rare CB-immunopositive cells (predominantly of the type 2) were observed almost exclusively in the GPl, close to its border with putamen (Fig. 5C). They were totally absent in the most rostral part of the GP.

Calretinin

Similarly to CB, CR staining was mainly observed in the neuropil. It consisted of a medium-to-dense pattern of immunoreactive puncta and fibers, present in both GPl and the GPm (Fig. 4I–L). It is worth noting that CR-ir clearly delineated the border between GPm and GPl (Figs 2L and 4J,K). In the GPl we observed various types of fibers. Laterally, parallel to the border with Pu, these fibers were long, thin and varicose (Fig. 5E). Such fibers were also observed in the medial part of GPl, although in that region there dominated bundles of thick, short and smooth fibers. A dense network of short, thin fibers with numerous varicosities was also present in the GPm (Fig. 5F). CR-ir cells were very scarce and observed exclusively in the GPl. All of them had small, oval cell bodies (Fig. 6C).

Table I

The distribution and density of CaBP immunoreactivity in the medial and lateral parts of globus pallidus of the opossum

Panel in Figure 1		A	B		C		D
Part of GP		GPl	GPl	GPm	GPl	GPm	GPl
PV	cells	++	+++	+++	+++	+++	++
	neuropil	•	••	••	••	••	•
CB	cells	-	+	+	+	+	+
	neuropil	•	•	•	•	•	•
CR	cells	+	+	+	+	+	+
	neuropil	••	••	•••	••	•••	••

The letters (A)–(D) refer to panels in Figure 1 presenting different levels of rostrocaudal extent of GP. The density of staining was assessed semi-quantatively as follows: (1) cells: (-) none; (+) light; (++) moderate; (+++) heavy; (2) neuropil (fibers and immunoreactive points): (•) sparse; (••) medium; (•••) dense.

Double-staining

Double immunohistochemistry allowed for assessment of colocalization of the three CaBPs within the GP. In general, the distribution and density pattern revealed by double staining mimicked that observed in single staining. Moreover, switching the fluorochromes in secondary antibodies did not influence the results. Most frequently, we observed the PV-ir cells to be scattered among CR-ir fibers or CB-ir puncta (Fig. 6A,B). We never observed more than one CaBP to be present in the same neuron of GP (Fig. 6). However, in GPl we observed CB-ir puncta surrounding the PV-ir cells (Fig. 6B).

DISCUSSION

Histology of the GP in Monodelphis, in comparison with other mammalian species

Our study describes for the first time the topography, divisions and heterogeneity of neurons in GP of the Monodelphis. In the Monotremes cells of the GP express predominantly parvalbumin, like in the opossum. In the echidna topography of the GP is similar to that in other mammals, while in the platypus it is expanded posteriorly, because of an unusual expansion of the ventral thalamic nuclei into the cerebral hemisphere in that species (Mikula et al. 2007). Earlier data on the GP in marsupials concern only the closely related opossum *Didelphis virginiana* (Bodian 1940, Loo 1930, Martin and Hamel 1967, Pilleri 1962, Schnitzlein et al. 1973, Tsai 1925). In that species authors analyzed the cytoarchitectonic of GP in the Nissl, Golgi and silver staining, morphology of its cells and some connections. The GP of Didelphis is described as a relatively small, pyramidal or globular nucleus. In Monodelphis it is elongated rostro-caudally as in rodents (Paxinos and Watson 1998). Its absolute size is smaller than in the rat, but proportional to the smaller body and brain size of the opossum (body weight 80–120 g, brain weight 0.8–1.1 g). The entopeduncular nucleus in Monodelphis is equally inconspicuous as in Didelphis.

As evaluated from the Nissl-stained sections (Figs 1 and 2), both parts of the Monodelphis GP are composed of medium-to-large triangular and large oval cells. However, in the GPm, the packing of the cells was visibly denser. Our findings are in agreement with the data of Pilleri (1962) for the rat, Martin and Hamel (1967) for the *Didelphis virginiana*, Schnitzlein and coauthors (1973) for bats and Hardman and others (2002) for the rat, marmoset, macaque, baboon and human. They found that morphology of the Nissl- or Golgi-stained neurons in the GP of various mammals and in the external part of GP in monkeys and humans (which is the homologue of the rat GP) is similar, and that the GP is built mainly of large, round and triangular neurons.

Divisions of GP in the opossum and other mammals

Some earlier investigators considered the GP to be a homogeneous structure. However, later authors variably divided it into: medial and lateral (rat – Sadek et al. 2007; humans – Levesque et al. 2003), dorsal and ventral (Didelphis – Mickle 1976; rat – Maurice et al. 1997, Naito and Kita 1994), anterior and posterior (rat – Shammah-Lagnado et al. 1996) or border (shell), middle and medio-caudal (rat – Gerfen et al. 1985, Kita and Kita 2001) parts. These divisions were based on various techniques and criteria. Generally, they point to inhomogeneity of the GP as concerning cell types and density, CaBPs expression, hodology and function.

Several histological techniques of staining that we employed in the two planes of sectioning unequivocally support its division into the lateral and medial parts (GPl and GPm, respectively). In both planes of sectioning the GPm is present only in the central part of the GP. The pattern of expression of the CaBPs also supports division of the Monodelphis GP into GPm and GPl, with very good agreement on the borders of these subnuclei. They were delineated most clearly in sections immunostained for PV and CR.

However, there were some further inhomogeneities in the GP revealed by immunolabeling for the CaBPs. Its border zone with the putamen has some unique properties, such as (1) the presence of a population of CB-expressing cells that were not observed in other parts of GP and (2) prevalence of a certain type of the CR-ir fibers (probably dendrites). Therefore, this part of the opossum GP may be homologous to the GP border (or shell) zone in the rat (Gerfen et al. 1985, Kita and Kita 2001). In that species, striatal axons projecting to GP have two separate terminal arbors: the first terminates within the border zone of the GP, while the second spreads in the central part of the GP, at a variable distance from the border (Chang et al 1981, Parent and Hazrati 1994). It is therefore possible that the border zone is another specialized part of the GP that was already present in the common ancestor of the Eutheria and Marsupials. Other inhomogeneities concern the lower density of PV-ir cells in the rostral and caudal poles of the GP. The physiological importance of these diferences may be clarified if the distribution of various afferents within the GP, targets of efferents of from various parts of GP and of various cell types, as well as the electrophysiological properties of its neurons are investigated.

Morphology of the GP neurons immunolabeled for the calcium binding proteins

Characteristics of the soma and dendritic tree of the opossum GP neurons expressing CaBP allowed us to distinguish three major morphological types. All three types were present among neurons immunolabeled for PV. The PV was expressed by a large proportion of GP neurons, while a very scarce population of neurons expressed CB or CR. What more, the CB-ir cells belonged mainly to the type 2 and all CR-ir cells belonged to type 3. These results are generally in agreement with findings of Rajakumar and colleagues (1994) and Cooper and Standford (2002) in the rat. They found that the PV-ir neurons were either fusiform or multipolar (similar to our types 1 and 2) while CB-ir neurons were bipolar or fusiform, resembling our type 2. The CR-ir neurons had small, oval-shaped soma, similarly to our type 3. Similar observations concerning the shape of PV-ir and CR-ir neurons were made in the squirrel monkeys (Fortin and Parent 1994, Parent et al. 1996). However, in that species the population of the CR-ir cells also included a type of large, multipolar neuron that was not observed in the rat or opossum. In the guinea pig three types of GP neurons, differing in electrophysiological characteristics, were found (Nambu and Llinas 1997). Thus, we can conclude that morphology of GP neurons expressing specific CaBPs is very similar across mammalian species.

Comparison of the distribution of neurons expressing CaBPs in the GP of the opossum and other mammals

Similarly to our findings in the opossum, several authors (Cooper and Stanford 2002, Hontanilla et al. 1998, Kita and Kitai 1994) observed a high density of the PV expressing neurons in the rat GP. PV was the main CaBP expressed in the GP of both rat and opossum. However, there is a difference in distribution between these two species. The biggest difference is in the distribution of PV-ir neurons in the GP. In the opossum it seems to be homogeneous throughout the nucleus, while in the rat their density is higher in the GPl (Cooper and Stanford 2002, Hardman et al. 2002, Hontanilla et al. 1998, Rajakumar et al. 1994). Similarly, density of the PV-expressing neurons in the external part of the primate GP, corresponding to the rat GP, is higher in its lateral part (monkey – Cote et al. 1991, Hardman et al. 2002,

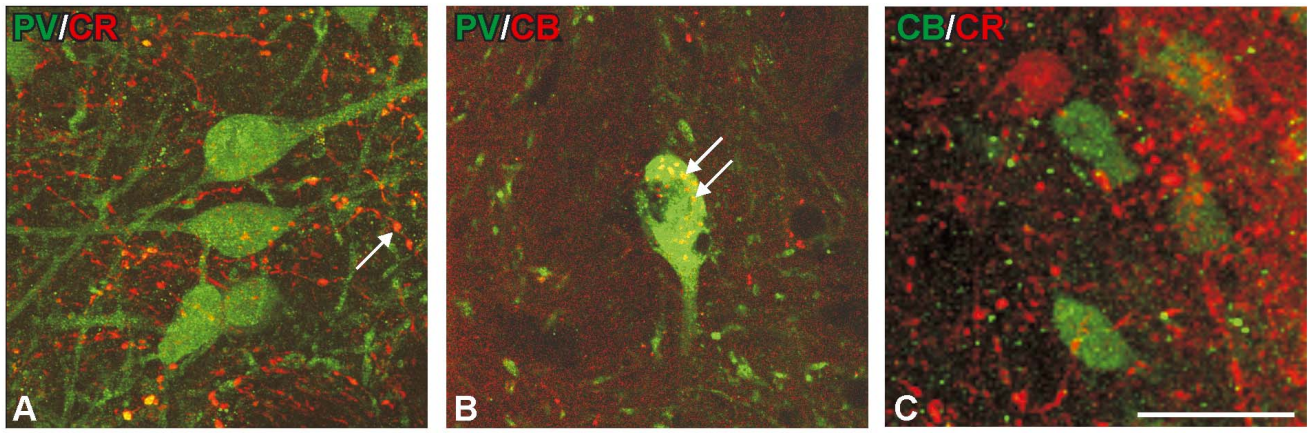

Fig. 6. Confocal microphotographs from section double-stained for (A) PV (green) and CR (red); (B) PV (green) and CB (red), and (C) CB (green) and CR (red). Arrows in panel (A) indicate varicosities on the CR-ir fiber. Arrows in (B) indicate CB-ir puncta on PV-ir cell. Scale bar in (C) equals to 25 μm and applies to (A)–(C).

Parent et al. 1996; human – Adams et al. 2001, Hardman et al. 2002, Kalanithi et al. 2005, Morel et al. 2002, Waldvogel et al. 1999, 2004). Although in the opossum we did not observe such a difference, we found that somata of the GPm neurons stained less intensely for PV than those of the GPl, which at first glance created an impression that the density of the PV-ir neurons in GPm is lower than in the GPl (compare panels B and C in Fig. 3). The same applies to PV-ir neuropil.

As in the rat and opossum, in the primates (marmoset, macaque, baboon and humans) large numbers of PV-ir cells were observed throughout the whole rostrocaudal level of GP (Adams et al. 2001, Cote et al. 1995, Hardman et al. 2002, Kalanithi et al. 2005, Morel et al. 2002, Waldvogel et al. 1999, 2004). Moreover, the proportion of GP neurons that express PV was consistent in the rat and primates (Hardman et al. 2002). In Monodelphis density of these cells decreased at the rostral and caudal poles of GP. It is possible that it reflects the general reduction of the cell density at the poles of GP.

In the opossum the CB-ir in neuropil was light and the single CB-ir cells were placed almost exclusively in the GPl, along its border with putamen. Density of the CB-ir neuropil was visibly higher in the GPm. In the rat, Cooper and Stanford (2002) also observed a high density of CB-ir neuropil, predominantly in the GPm, but also numerous CB-ir cells, mostly in the GPl, close to its border with putamen. Hontanilla and coauthors (1998) also found that the CB-ir neuropil was dense in the rat GP, with a higher density in the GPm, but in their study the density of CB-ir neurons was classified as low. In the squirrel monkey Cote and colleagues (1995) did not observe any CB-ir neurons, in contrast to intensely stained neuropil. Similar observations have been made in humans (Morel et al 2002, Waldvogel et al. 1999). Therefore, the CB-ir elements in the opossum GP are more similar to those observed in the rat than in the primates.

We observed only single CR-ir neurons scattered in the opossum GPm and GPl. Cooper and Stanford (2002) made similar observations in the rat. They postulated also that the CR is a marker for the GP interneurons. This statement was additionally supported by electrophysiological, morphological and neurochemical data (Millhouse 1986, Nambu and Llinas 1997, Standaert et al. 1996). Similar conclusion about CR being a marker of interneurons was drawn by Waldvogel and coauthors (2004) in humans, although there the CR-ir neurons were numerous. If the CR-ir cells are indeed interneurons, we can conclude that either in the rat and opossum (unlike in primates) the GP contains a low proportion of interneurons, or interneurons in these species rarely express CR.

In both rat (Cooper and Stanford 2002) and opossum (present data) neuropil staining for CR was intense in the whole GP, but it was denser in GPm. Furthermore, in the GPl, unlike in the GPm, the CR-ir fibers were long, thin and parallel to the border with putamen. In contrast to the rat and opossum, CR immunoreactivity of neuropil in the primates was classified as light (Parent et al. 1996, Waldvogel et al. 1999) and few CR-ir neurons were observed.

Lack of CaBPs colocalization in neurons of the Monodelphis GP

Similarly to what was observed in the rat (Cooper and Stanford 2002), in the opossum we never observed colocalization of PV, CR and/or CB immunoreactivity within the same cell. In contrast, the study of Waldvogel and coauthors (1999) in humans described colocalization of the PV and CR immunoreactivity in large neurons of the external segments of the GP. It is important to note that this type of large CR-ir neurons expressing both PV and CR seems to be characteristic only for the human GP.

Our study is also the first to describe the CB-ir puncta forming basket-like structures surrounding PV-ir cells in the opossum GPl. This may mean that neurons expressing CB project on the PV-ir neurons. Cooper and Stanford (2002) used retrograde tracing of the projection neurons and immunolabeling for CaBP in the rat and showed that projection neurons of the rat GP express either CB or PV. As was previously mentioned, CR is a good marker of the GP interneurons. Because we never observed colocalization of CR with either CB or PV we can speculate that the CB-ir baskets around PV-ir cells are a part of specific loops formed by neurons projecting to GP from other structures.

Therefore, our results show that placement and histology of the Monodelphis GP is very similar to those described in other mammals, with the highest similarity to what we find in Didelphis and rodents. Distribution and density of the CaBP in the opossum GP generally follows the pattern observed in the rat, however some unique features are also observed. In comparison with primate we find many similarities, but also a higher number of differences.

Functional implications

Several morphological and intracellular studies combined with electrophysiology revealed the existence of various neuronal subtypes within GP (Iwahori and Mizuno 1981, Kita and Kitai 1991, 1994, Park et al. 1982). Also *in vivo* studies identified multiple subtypes of the GP neurons on the basis of the firing pattern and waveform (Cooper and Stanford 2000, Kita and Kitai 1991). However, expression of a particular CaBP in the GP neuron does not appear to be linked with a particular neurotransmitter used by that neuron. For example, PV expression has been observed in the GABA-ergic, glycinergic and glutamatergic neurons (cf. for review Baimbridge et al. 1992). However, the PV expression has been linked with the fast-spiking type (Kawaguchi et al. 1995). What is more, it is possible that CR is expressed exclusively by the GP interneurons. Therefore, we can speculate that differences in the distribution of CaBPs in GP neurons may reflect the heterogeneity of its neuronal population, as revealed by electrophysiological studies. This heterogeneity may be linked with differences in the connectivity and therefore have functional implications. This hypothesis remains to be tested.

CONCLUSIONS

This first detailed description of GP in the marsupials showed that in the opossum *Monodelphis domestica* GP is a small nucleus placed between the striatum and internal capsule. It consists of the medial and lateral parts that are visible in sections stained with several methods. Many GP neurons express PV and only few of them express CB or CR, with no colocalization of these proteins. The PV-ir neurons form a heterogeneous group that was classified into three morphological types. Density of the PV-immunopositive fibers and puncta correlated with the density of PV-immunolabeled neurons, while labeling for CB or CR resulted mainly in staining of the neuropil. The CB-immunoreactive puncta frequently formed basket-like structures around the PV-immunoreactive neurons. Therefore, GP of the opossum consists of a diversified population of neurons and afferents, probably playing various functions. These morphological characteristics of GP are closer to those in the rat, than in the primates.

ACKNOWLEDGEMENTS

This study was supported by funds from the Polish Ministry of Science and Higher Education Grant ST-11 to Gdańsk Medical University and grant Nr 0697/P05/2005/29. We are grateful to R. Doty and K. Ashwell for valuable comments and corrections.

REFERENCES

Adams I, Brauer K, Arelin C, Hartig W, Fine A, Mader M, Arendt T, Bruckner G (2001) Perineuronal nets in the rhesus monkey and human basal forebrain including basal ganglia. Neuroscience 108: 285–298.

Badowska-Szalewska E, Klejbor I, Ludkiewicz B, Morys J (2005) Analysis of calretinin immunoreactivity in the rat piriform cortex after open field stress during postnatal maturation. Folia Morphol (Warsz) 64: 33–40.

Baimbridge KG, Celio MR, Rogers JH (1992) Calcium-binding proteins in the nervous system. Trends Neurosci 15: 303–308.

Bano D, Nicotera P (2007) Ca2+ signals and neuronal death in brain ischemia. Stroke 38: 674–676.

Barker DA, Dreher B (1998) Spatiotemporal patterns of ontogenetic expression of parvalbumin in the superior colliculi of rats and rabbits. J Comp Neurol 393: 210–30.

Beck PD, Pospichal MW, Kaas JH (1996) Topography, architecture, and connections of somatosensory cortex in opossums: evidence for five somatosensory areas. J Comp Neurol 366: 109–133.

Bevan MD, Booth PA, Eaton SA, Bolam JP (1998) Selective innervation of neostriatal interneurons by a subclass of neuron in the globus pallidus of the rat. J Neurosci 18: 9438–9452.

Bodian D (1940) Studies on the diencephalons of the Virginia opossum. II. The fiber connections in normal and experimental material. J Comp Neurol 72: 207–297.

Burgoyne RD (2007) Neuronal calcium sensor proteins: generating diversity in neuronal Ca2+ signalling. Nat Rev Neurosci 8: 182–193.

Calder AJ, Beaver JD, Davis MH, van Ditzhuijzen J, Keane J, Lawrence AD (2007) Disgust sensitivity predicts the insula and pallidal response to pictures of disgusting foods. Eur J Neurosci 25: 3422–3428.

Celio MR (1990) Calbindin D-28k and parvalbumin in the rat nervous system. Neuroscience 35: 375–475.

Chang HT, Wilson CJ, Kitai ST (1981) Single neostriatal efferent axons in the globus pallidus: A light and electron microscopic study. Science 213: 915–918.

Cheng G, Marotte LR, Ashwell KW (2003) Cyto-and chemoarchitecture of the hypothalamus of a wallaby (Macropus eugenii) with special emphasis on oxytocin and vasopressinergic neurons. Anat Embryol (Berl) 207: 233–253.

Cooper AJ, Stanford IM (2000) Electrophysiological and morphological characteristics of three subtypes of rat globus pallidus neurone in vitro. J.Physiol 527 Pt 2: 291–304.

Cooper AJ, Stanford IM (2002) Calbindin D-28k positive projection neurones and calretinin positive interneurones of the rat globus pallidus. Brain Res. 929: 243–251.

Cote PY, Sadikot AF, Parent A (1991) Complementary distribution of calbindin D-28k and parvalbumin in the basal forebrain and midbrain of the squirrel monkey. Eur J Neurosci 3: 1316–1329.

Cote PY, Levitt P, Parent A (1995) Distribution of limbic system-associated membrane protein immunoreactivity in primate basal ganglia. Neuroscience 69: 71–81.

Danscher G (1981) Histochemical demonstration of heavy metals. A revised version of the sulphide silver method suitable for both light and electronmicroscopy. Histochemistry 71: 1–16.

Difiglia M, Rafols JA (1988) Synaptic organization of the globus pallidus. J Electron Microsc Tech 10: 247–263.

Difiglia M, Pasik P, Pasik T (1982) A Golgi and ultrastructural study of the monkey globus pallidus. J Comp Neurol 212: 53–75.

Dino MR, Willard FH, Mugnaini E (1999) Distribution of unipolar brush cells and other calretinin immunoreactive components in the mammalian cerebellar cortex. J Neurocytol 28: 99–123.

Djavadian R, Bisti S, Maccarone R, Bartkowska K, Turlejski K (2006) Development and plasticity of the retina in the opossum Monodelphis domestica. Acta Neurobiol Exp (Wars) 66: 179–188.

FitzGibbon T, Solomon SG, Goodchild AK (2000) Distribution of calbindin, parvalbumin, and calretinin immunoreactivity in the reticular thalamic nucleus of the marmoset: evidence for a medial leaflet of incertal neurons. Exp Neurol 164: 371–383.

Fortin M, Parent A (1994) Calretinin labels a specific neuronal subpopulation in primate globus pallidus. Neuroreport 5: 2097–2100.

Frost SB, Milliken GW, Plautz EJ, Masterton RB, Nudo RJ (2000) Somatosensory and motor representations in cerebral cortex of a primitive mammal (Monodelphis domestica): a window into the early evolution of sensorimotor cortex. J Comp Neurol 421: 29–51.

Gerfen CR (2004) Basal ganglia. In: The Rat Nervous System (Third Edition). Elsevier, Academic Press, Amsterdam, pp. 455–508.

Gerfen CR, Baimbridge KG, Miller JJ (1985) The neostriatal mosaic: Compartmental distribution of calcium-binding protein and parvalbumin in the basal ganglia of the rat and monkey. Proc Natl Acad Sci U S A 82: 8780–8784.

Grove EA, Domesick VB, Nauta WJH (1986). Light microscopic evidence of striatal input to intrapallidal neurons of cholinergic cell group Ch4 in the rat: A study employing the anterograde tracer Phaseolus vulgaris leucagglutinin (PHA-L). Brain Res 367: 379–384.

Haber SN, Groenewegen HJ, Grove EA, Nauta WJ (1985). Efferent connections of the ventral pallidum: evidence of a dual striato pallidofugal pathway. J Comp Neurol 235: 322–335.

Haber SN, Lynd-Balta E, Mitchell SJ (1993) The organization of the descending ventral pallidal projections in the monkey J Comp Neurol 329: 111–128.

Hamel EG Jr (1966) A study of the hippocampal formation in the opossum, Didelphis virginiana. In: Evolution of the Forebrain (Hassler R, Stephan H, Eds). Georg Thieme Verlag, Stuttgart, pp. 81–91.

Hardman CD, Henderson JM, Finkelstein DI, Horne MK, Paxinos G, Halliday GM (2002) Comparison of the basal ganglia in rats, marmosets, macaques, baboons, and humans: volume and neuronal number for the output, internal relay, and striatal modulating nuclei. J Comp Neurol 445: 238–255.

Heath CJ, Jones EG (1971) Interhemispheric pathways in the absence of a corpus callosum. An experimental study of commissural connexions in the marsupial phalanger. J Anat 109: 253–270.

Heizmann CW, Braun K (1992) Changes in Ca(2+)-binding proteins in human neurodegenerative disorders. Trends Neurosci 15: 259–264.

Hof PR, Glezer II, Conde F, Flagg RA, Rubin MB, Nimchinsky EA, Vogt Weisenhorn DM (1999) Cellular distribution of the calcium-binding proteins parvalbumin, calbindin, and calretinin in the neocortex of mammals: phylogenetic and developmental patterns. J Chem Neuroanat 16: 77–116.

Hontanilla B, Parent A, de las HS, Gimenez-Amaya JM (1998) Distribution of calbindin D-28k and parvalbumin neurons and fibers in the rat basal ganglia. Brain Res Bull 47: 107–116.

Hooks MS, Kalivas PW (1995) The role of mesoaccumbens-pallidal circuitry in novelty-induced behavioral activation. Neuroscience 64: 587–597.

Hoover BR, Marshall JF (2002) Further characterization of preproenkephalin mRNA-containing cells in the rodent globus pallidus. Neuroscience 111: 111–125.

Ingham CA, Bolam JP, Wainer BH, Smith AD (1985) A correlated light and electron microscopic study of identified cholinergic basal forebrain neurons that project to the cortex in the rat. J Comp Neurol 239: 176–192.

Iwahori N, Mizuno N (1981) A Golgi study on the globus pallidus of the mouse. J Comp Neurol 197: 29–43.

Jia C, Halpern M (2004) Calbindin D28k, parvalbumin, and calretinin immunoreactivity in the main and accessory olfactory bulbs of the gray short-tailed opossum, Monodelphis domestica. J Morphol 259: 271–280.

Jones EG (2007) The Thalamus (2nd ed.) Cambridge University Press, Cambridge, UK.

Kalanithi PS, Zheng W, Kataoka Y, DiFiglia M, Grantz H, Saper CB, Schwartz ML, Leckman JF, Vaccarino FM (2005) Altered parvalbumin-positive neuron distribution in basal ganglia of individuals with Tourette syndrome. Proc Natl Acad Sci U S A 102: 13307–13312.

Kalivas PW, Churchill L, Romanides A (1999) Involvement of the pallidal-thalamocortical circuit in adaptive behavior. Ann N Y Acad Sci 877: 64–70.

Karlen SJ, Krubitzer L (2006) Phenotypic diversity is the cornerstone of evolution: variation in cortical field size within short-tailed opossums. J Comp Neurol 499: 990–999.

Karlen SJ, Krubitzer L (2007) The functional and anatomical organization of marsupial neocortex: Evidence for parallel evolution across mammals. Prog Neurobiol 82: 122–141.

Kawaguchi Y, Wilson CJ, Augood SJ, Emson PC (1995) Striatal interneurones: chemical, physiological and morphological characterization. Trends Neurosci 18: 527–535. [Erratum in Trends Neurosci 19: 143.]

Kincaid AE, Penney JB Jr, Young AB, Newman SW (1991) Evidence for a projection from the globus pallidus to the entopeduncular nucleus in the rat. Neurosci Lett 128: 121–125.

Kita H (2007) Globus pallidus external segment. Prog Brain Res 160: 111–133.

Kita H, Kita T (2001) Number, origins, and chemical types of rat pallidostriatal projection neurons. J Comp Neurol 437: 438–448.

Kita H, Kitai ST (1987) Efferent projections of the subthalamic nucleus in the rat: Light and electron microscopic analysis with the PHA-L method. J Comp Neurol 260: 435–452.

Kita H, Kitai ST (1991) Intracellular study of rat globus pallidus neurons: membrane properties and responses to neostriatal, subthalamic and nigral stimulation. Brain Res 564: 296–305.

Kita H, Kitai ST (1994) The morphology of globus pallidus projection neurons in the rat: an intracellular staining study. Brain Res 636: 308–319.

Krause WJ, Saunders NR (1994) Brain growth and neocortical development in the opossum. Ann Anat 176:395–407.

Lende RA (1963a) Sensory representation in the cerebral cortex of the opossum (Didelphis virginiana). J Comp Neurol 121: 395–403.

Lende RA (1963b) Motor representation in the cerebral cortex of the opossum (Didelphis virginiana). J Comp Neurol 121: 405-415.

Levesque M, Bedard A, Cossette M, Parent A (2003) Novel aspects of the chemical anatomy of the striatum and its efferents projections. J Chem Neuroanat 26: 271–281.

Loo YT (1930) The forebrain of the opossum, Didelphis virginiana. Part I. Gross anatomy. J Comp Neurol 51: 13–64.

Loo YT (1931) The forebrain of the opossum, Didelphis virginiana. Part II. Histology. J Comp Neurol 52: 1–148.

Martin GF Jr, Hamel EG Jr (1967) The striatum of the opossum, Didelphis virginiana. Description and experimental studies. J Comp Neurol 131: 491–516.

Mattson MP (2007) Calcium and neurodegeneration. Aging Cell 6: 337–350.

Maurice N, Deniau JM, Menetrey A, Glowinski J, Thierry AM (1997) Position of the ventral pallidum in the rat prefrontal cortex-basal ganglia circuit. Neuroscience 80: 523–534.

Mickle JP (1976) Efferent connections of the caudate nucleus in the Virginia opossum. J Comp Neurol 166: 373–385.

Mikula S, Manger PR, Jones EG (2007) The thalamus of the monotremes: cyto- and myeloarchitecture and chemical neuroanatomy. Phil Trans R Soc B (Epub ahead of print May 19, 2007).

Millhouse OE (1986) Pallidal neurons in the rat. J Comp Neurol 254: 209–227.

Morel A, Loup F, Magnin M, Jeanmonod D (2002) Neurochemical organization of the human basal ganglia: anatomofunctional territories defined by the distributions of calcium-binding proteins and SMI-32. J Comp Neurol 443: 86–103.

Moriizumi T, Hattori T (1992) Ultrastructural morphology of projections from the medial geniculate nucleus and its adjacent region to the basal ganglia. Brain Res Bull 29: 193–198.

Naito A, Kita H (1994) The cortico-pallidal projection in the rat: an anterograde tracing study with biotinylated dextran amine. Brain Res 653: 251–257.

Nambu A (2007) Globus pallidus internal segment. Prog Brain Res 160: 135–150.

Nambu A, Llinas R (1994) Electrophysiology of globus pallidus neurons in vitro. J Neurophysiol 72: 1127–1139.

Nambu A, Llinas R (1997) Morphology of globus pallidus neurones: its correlation with electrophysiology in guinea pig brain slices. J Comp Neurol 377: 85–94.

Oswaldo-Cruz E, Rocha-Miranda CE (1968) The Brain of the Opossum (Didelphis marsupialis): A Cytoarchitectonic Atlas in Stereotaxic Coordinates. Instituto de Biofisica Universida de Federal do Rio de Janeiro, pp.1–99.

Paxinos G, Watson C (1998) The Rat Brain in Stereotaxic Coordinates, 4th Edition. Academic Press, San Diego, CA.

Parent A, Hazrati LN (1994) Multiple striatal representation in primate substantia nigra. J Comp Neurol 344: 305–320.

Parent A, Fortin M, Cote PY, Cicchetti F (1996) Calcium-binding proteins in primate basal ganglia. Neurosci Res 25: 309–334.

Park MR, Falls WM, Kitai ST (1982) An intracellular HRP study of the rat globus pallidus. I. Responses and light microscopic analysis. J Comp Neurol 211: 284–294.

Pilleri G (1962) On the fine structure and comparative anatomy of the corpus striatum of primitive marsupials and rodents (in German). Acta Anat (Basel) 48: 347–367.

Pubols BH, Jr., Pubols LM, DiPette DJ, Sheely JC (1976) Opossum somatic sensory cortex: a microelectrode mapping study. J Comp Neurol 165: 229–245.

Rajakumar N, Rushlow W, Naus CC, Elisevich K, Flumerfelt BA (1994) Neurochemical compartmentalization of the globus pallidus in the rat: an immunocytochemical study of calcium-binding proteins. J Comp Neurol 346: 337–348.

Resibois A, Rogers JH (1992) Calretinin in rat brain: an immunohistochemical study. Neuroscience 46: 101–134.

Rowe MH, Wilson PD, Rapaport DH (1981) Conduction of velocity groups in the optic nerve of the North American opossum (Didelphis virginiana): retinal origins and central projections. J.Comp Neurol 199: 481–493.

Sadek AR, Magill PJ, Bolam JP (2007) A single-cell analysis of intrinsic connectivity in the rat globus pallidus. J Neurosci 27: 6352–6362.

Saunders NR, Adam E, Reader M, Mollgard K (1989) Monodelphis domestica (grey short-tailed opossum): an accessible model for studies of early neocortical development. Anat Embryol (Berl) 180: 227–236.

Schnitzlein HN, Hamel EG Jr, Carey JH, Brown JW, Hoffman HH, Faucette JR, Showers MJ (1973) The interrelations of the striatum with subcortical areas through the lateral forebrain bundle. J Hirnforsch 13: 409–455.

Shammah-Lagnado SJ, Alheid GF, Heimer L (1996) Efferent connections of the caudal part of the globus pallidus in the rat. J Comp Neurol 376: 489–507.

Smith Y, Bolam JP (1989) Neurons of the substantia nigra reticulata receive a dense GABA-containing input from the globus pallidus in the rat. Brain Res 493: 160–167.

Standaert DG, Landwehrmeyer GB, Kerner JA, Penney JB, Jr., Young AB (1996) Expression of NMDAR2D glutamate receptor subunit mRNA in neurochemically identified interneurons in the rat neostriatum, neocortex and hippocampus. Mol.Brain Res 42: 89–102.

Stepniewska I, Preuss TM, Kaas JH (2007) Thalamic connections of the dorsal and ventral premotor areas in New World owl monkeys. Neuroscience 147: 727–745.

Tsai C (1925) The optic tracts and centers of the opossum, Didelphis virginiana. J Comp Neurol 39: 173-216.

Waldvogel HJ, Kubota Y, Fritschy J, Mohler H, Faull RL (1999) Regional and cellular localisation of GABA(A) receptor subunits in the human basal ganglia: An autoradiographic and immunohistochemical study. J Comp Neurol 415: 313–340.

Waldvogel HJ, Billinton A, White JH, Emson PC, Faull RL (2004) Comparative cellular distribution of GABAA and GABAB receptors in the human basal ganglia: immunohistochemical colocalization of the alpha 1 subunit of the GABAA receptor, and the GABABR1 and GABABR2 receptor subunits. J Comp Neurol 470: 339–356.

Wojcik S, Dziewiatkowski J, Klejbor I, Spodnik JH, Kowianski P, Morys J (2006) The anatomical relationships between the serotonergic afferents and the neurons containing calcium-binding proteins in the rat claustrum. Acta Neurobiol Exp (Wars) 66: 33–42.

Xue Y, Chen L, Cui QL, Xie JX, Yung WH (2007) Electrophysiological and behavioral effects of neurotensin in rat globus pallidus: an in vivo study. Exp Neurol 205: 108–115.

Zold CL, Larramendy C, Riquelme LA, Murer MG (2007) Distinct changes in evoked and resting globus pallidus activity in early and late Parkinson's disease experimental models. Eur J Neurosci 26: 1267–1279.

Received 15 September 2007, accepted 19 October 2007